Polymer 51 (2010) 5207–5211

Contents lists available at ScienceDirect

Polymer

journal homepage: www.elsevier.com/locate/polymer

Dynamic mechanical behaviour of polyamide 11/Barium titanate ferroelectric composites

Jean-Fabien Capsal, Chloé Pousserot, Eric Dantras*, Jany Dandurand, Colette Lacabanne

Physique des Polymères, Institut CARNOT-CIRIMAT, Université Paul Sabatier, 31062 Toulouse cedex 09, France

ARTICLE INFO

Article history:
Received 2 April 2010
Received in revised form
1 September 2010
Accepted 2 September 2010
Available online 15 September 2010

Keywords:
Mechanical behaviour
Nanocomposite
Polymer

ABSTRACT

Dynamic mechanical analysis and tensile test have been used to characterize the mechanical behaviour of hybrid composites. Barium titanate ($BaTiO_3$) is the submicron filler and polyamide 11 (PA 11) the matrix. The influence of volume fraction and particles size (ranging from 100 nm to 700 nm) of the inorganic phase on the composites mechanical properties have been checked. $BaTiO_3$ dispersion in the matrix increases the tensile modulus of the composites and an evolution from ductile to fragile is observed for volume fractions above 12 vol%. The volume fraction dependence of the glassy shear modulus is well described by the Hashin and Shtrikman model indicative of an interaction lack between the organic and inorganic phases. The decrease of the glassy shear modulus with the filler size has been associated with the existence of softer organic/inorganic interfaces, in agreement with the previous hypothesis. The non linear variation of the rubbery modulus versus particles content is well described by the rubber elasticity model applied to a hydrogen bond network.

1. Introduction

In the past decades, a great interest has been devoted to ferroelectric polymers due to their attractive morphology and engineering behaviour [1,2]. Nevertheless, ferroelectric ceramics have easier poling conditions and higher ferroelectric activity [3]. Hybrid composites tend to associate these advantages, but, due to the difference of dielectric permittivity between polymer and ceramic, hybrid composites have to be filled with high volume ratio to ensure measurable electroactive properties [4,5]. Consequently, they loose the mechanical characteristics of the matrix.

So hybrid composites were proposed to overcome this inconvenience. For this purpose, ferroelectric inorganic nanofillers have been dispersed in a polymer in order to obtain 0–3 composites according to the Newnham nomenclature [6]. Due to its interesting mechanical properties, polyamide has been widely used as matrix of composites with organic or inorganic fillers but generally, the objective is the optimization of mechanical properties [7,8]. In this work, the challenge is to use modest BT contents to keep satisfactory mechanical performances while permitting to reach measurable electroactive properties. Since these materials have potential applications in force sensors [9] or electromechanical transduction [10], it is crucial to evaluate the influence of filler on the mechanical behaviour of the matrix.

Few works have been devoted to the nanoceramic influence on mechanical properties of ferroelectric composites [11,12]. As far as we know, a complete mechanical study of such materials as a function of submicron particles size has not yet been reported. In previous works [13,14], the ferroelectric properties of polyamide 11/nano-$BaTiO_3$ composites have been studied as a function of size and volume fraction. The piezoelectric coefficient decreases drastically for particles diameter below 100 nm. Consequently, $BaTiO_3$ particles ranging from 100 nm to 700 nm and volume fractions from 0 to 58 vol% have been used for this work.

In this paper we focus on the shear and tensile mechanical behaviour of these composites. The influence of the $BaTiO_3$ volume fraction has been studied using 700 nm particles. The particles size influence has been studied for PA11/$BaTiO_3$ with $\varphi = 12\%$ in order to maintain constant the connectivity state in the composite.

2. Experimental

2.1. Elaboration

The mean diameter of $BaTiO_3$ (BT) was 700 nm, 300 nm and 100 nm. PA11 powder was dissolved in a solution of Dimethyl Acetyl Amide (DMAc) and the required $BaTiO_3$ was dispersed by ultrasonic stirring, in order to form a homogeneous suspension. The samples were dried over night at 140 °C to remove solvent traces. Then, the composites were hot pressed at 220 °C to form 4 cm × 1 cm × 1 mm rectangular samples. The volume fraction of

* Corresponding author.
E-mail address: dantras@cict.fr (E. Dantras).

0032-3861/$ – see front matter © 2010 Elsevier Ltd. All rights reserved.
doi:10.1016/j.polymer.2010.09.011

BT was determined by density measurements from the following mixture law:

$$d_{composite} = (1-\varphi)d_{PA11} + \varphi d_{BT} \quad (1)$$

where $d_{PA11} = 1.05$, $d_{BT} = 6.05$ and φ is the volume ratio. In composites, φ is ranging from 0 to 58%.

2.2. Characterization

Standard differential scanning calorimetry (DSC) measurements were performed using a DSC/TMDSC 2920 set up. The sample temperature was calibrated using the onset of melting of tin (T_m = 231.88 °C), indium (T_m = 156.6 °C) and cyclohexane (T_m = 6 °C) with a heating rate of $q_h = +5$ °C.min^{-1}. The heat-flow was calibrated with the heat fusion of indium ($\Delta H = 28.45$ J g^{-1}), its baseline was corrected with sapphire. DSC experiments were systematically carried out over a temperature range from the equilibrium state (in order to remove the effect of previous thermal history) $T_{eq} = T_m + 20$ °C down to the glassy state $T_0 = T_g - 70$ °C with a constant cooling rate $q_c = +20$ °C min^{-1}, and followed by a linear heating rate $q_h = 10$ °C min^{-1}.

In Fig. 1, the DSC thermograms of PA11/$BaTiO_3$ composites are reported. In the temperature range 180–190 °C, an endothermic phenomenon is pointed out. It has been attributed to the melting of PA11 crystalline phase. The crystalline ratio χ_c of composites has been extracted from these thermograms and reported as function of the BT volume fraction in the insert of Fig. 1. A mild decrease of 3% for $\varphi = 58\%$ is observed.

2.3. Mechanical analysis

Tensile stress–strain experiments were performed at 25 °C using a Hounsfield tensile tension machine. For recording stress–strain measurements, an extensional rate of 0.5 mm min^{-1} was employed.

Dynamic Mechanical Analyses (DMA) were performed on an ARES (Advanced Rheometric Expansion System) strain controlled rheometer (TA Instruments) in the torsion rectangular mode within the linear elasticity range (0.1% strain at a frequency of 1 rad s^{-1}). Dynamic mechanical storage and dissipative moduli (G' and G'') were measured as a function of temperature and BT content from − 100 to 100 °C at 1 °C/min. The shear modulus $G^*(T)$ has been characterized for various volume fraction and BT particles size. The storage modulus G' (T) versus volume fraction and BT size is reported in Fig. 2 and Fig. 3 respectively. In the low temperature range i.e; near $T_\beta = -80$ °C a weak relaxation mode called β, can be detected in Fig. 2. According with the literature [15], it has been attributed to the mechanical relaxation of water–amide complexes. The primary relaxation mode labelled α, centred on $T_\alpha = 35$ °C, is associated with the mechanical manifestation of the polyamide 11 glass transition. For PA11, in the viscoelastic region, G' decreases from 450 MPa to 70 MPa.

3. Results and discussion

3.1. Plasticity

The tensile mechanical behaviour of PA11/$BaTiO_3$ 700 nm composites has been characterized by longitudinal traction experiments. The volume fraction increases from 0 to 45%. The maximum stress, σ_{max}, decreases with increasing ceramic ratio; from 36 MPa for PA11 to 22 MPa for 45 vol% BT. The strain at break (ε_{break}) decreases with volume fraction. ε_{break} is ranging from 175% (PA11) to 1.43% for 45 vol% BT. The decrease of ε_{break} is indicative of the evolution of the composites mechanical behaviour. The stress/strain behaviour is reported in Fig. 4. The composites have a ductile behaviour until 12 vol%. Above $\varphi = 12\%$, composites are characterized by a fragile behaviour. The ductile behaviour of polyamide 11 is maintained until this critical value. Fig. 4 shows that the slope of σ (ε), associated with the E tensile modulus, increases with the volume fraction of BT. The introduction of $BaTiO_3$ submicron particles hardens the composite due to the high tensile modulus of the inorganic phase compared to the organic one.

The stress/strain curves of composites with particles size of 100 nm, 300 nm and 700 nm are shown in Fig. 5 for two volume fractions (12% and 24%). For a constant volume fraction, the global tensile behaviour is independent from BT particles size. PA11/$BaTiO_3$ composites with $\varphi = 12\%$ show a plasticity threshold independently of particles size. The maximum stress, the stress at break and the strain at plasticity threshold are also filler size independent. However, the strain at break of composites elaborated with 100 nm and 300 nm $BaTiO_3$ is slightly lower than ε_{break} of PA11/$BaTiO_3$ 700 nm. A fragile mechanical behaviour is observed for $\varphi = 24\%$. These composites break at a tensile stress of 25 MPa and a tensile strain of 3%.

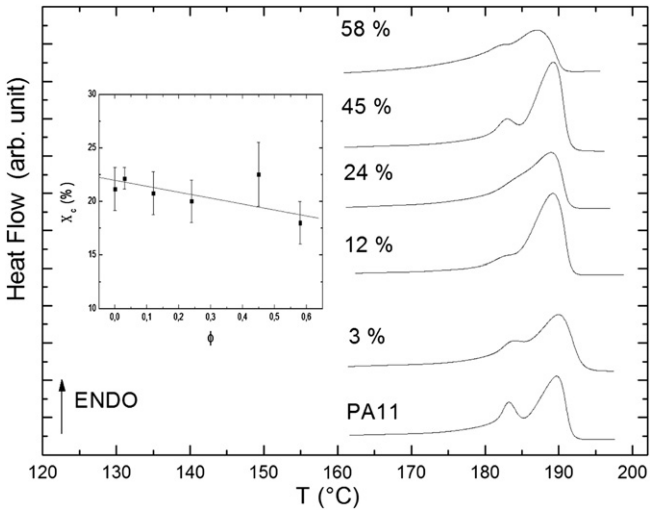

Fig. 1. Differential scanning calorimetry thermograms of PA11/$BaTiO_3$ 700 nm composites with φ ranging from 0 to 58% and crystalline degree versus volume fraction of $BaTiO_3$ in insert.

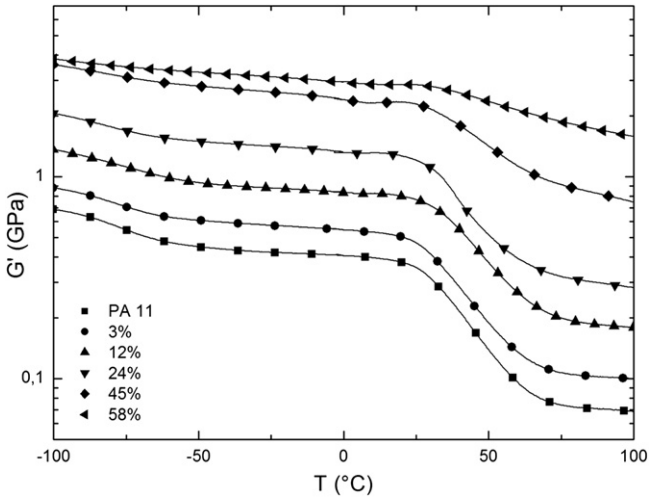

Fig. 2. Storage shear modulus G' versus temperature T for PA11/$BaTiO_3$, 700 nm composites.

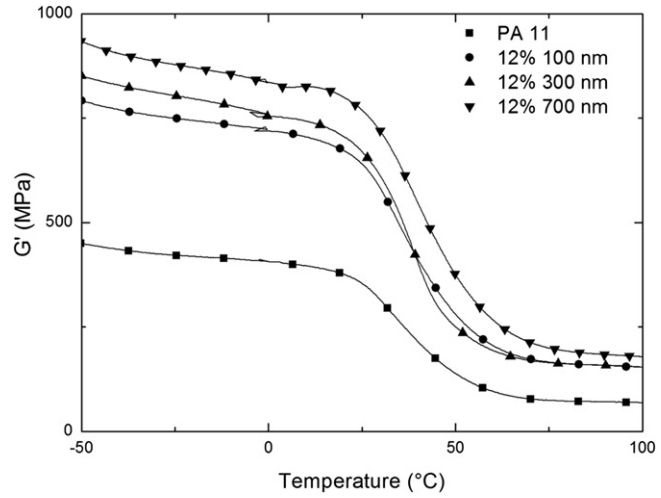

Fig. 3. Storage shear modulus G′ versus temperature T for PA11/$BaTiO_3$ with $\varphi = 12\%$ and particles size of 100 nm, 300 nm, 700 nm.

The evolution with φ of the mechanical behaviour has been associated with the increase of heterogeneities in the vitreous phase.

3.2. Rubbery plateau

The influence of the BT volume fraction on the storage shear modulus in the viscoelastic state is reported in Fig. 6-a. BT particles increase the value of G' on the rubbery plateau. This increase of G_R with the filler content is in good agreement with several authors [16–19]: a non linear evolution with φ is observed. The BT particles are dispersed in the amorphous phase of PA11. Above T_α, the amorphous phase is in a liquid state and the mechanical behaviour is assumed to be mostly governed by the crystalline phase. The influence of inorganic content on PA 11 crystallinity is weak so that the increase of G_R cannot be attributed to the crystalline phase evolution. Several factors may contribute to the increase of the rubbery plateau modulus with the BT content: reinforcing effect by the fillers, decrease of the molecular mobility due to physical interactions between inorganic and organic phases and decrease of the matrix number-average molecular weight between hydrogen bonds. On the one hand, the non linear evolution of G_R with the

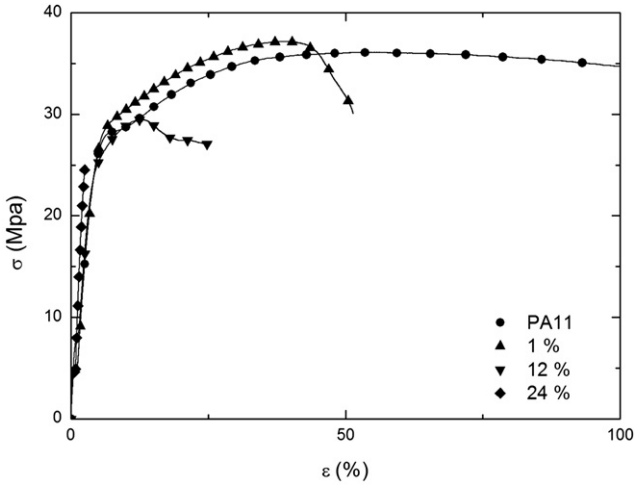

Fig. 4. Stress (σ) versus strain (ε) curves of PA11/$BaTiO_3$ 700 nm composites with φ ranging from 0 to 24 vol%.

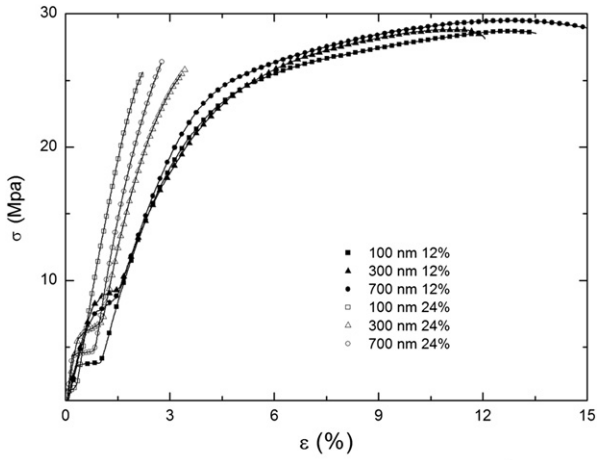

Fig. 5. Stress (σ) versus strain (ε) curves of PA11/$BaTiO_3$ composites with $\varphi = 12\%$ and 24% and fillers size of 100 nm, 300 nm and 700 nm.

filler indicates that reinforcing effect is a minor parameter for explaining the rubbery stiffness. On the other hand, several studies have reported the influence of fillers/polymer interactions on the vitreous transition temperature [20–23]. The constant viscoelastic

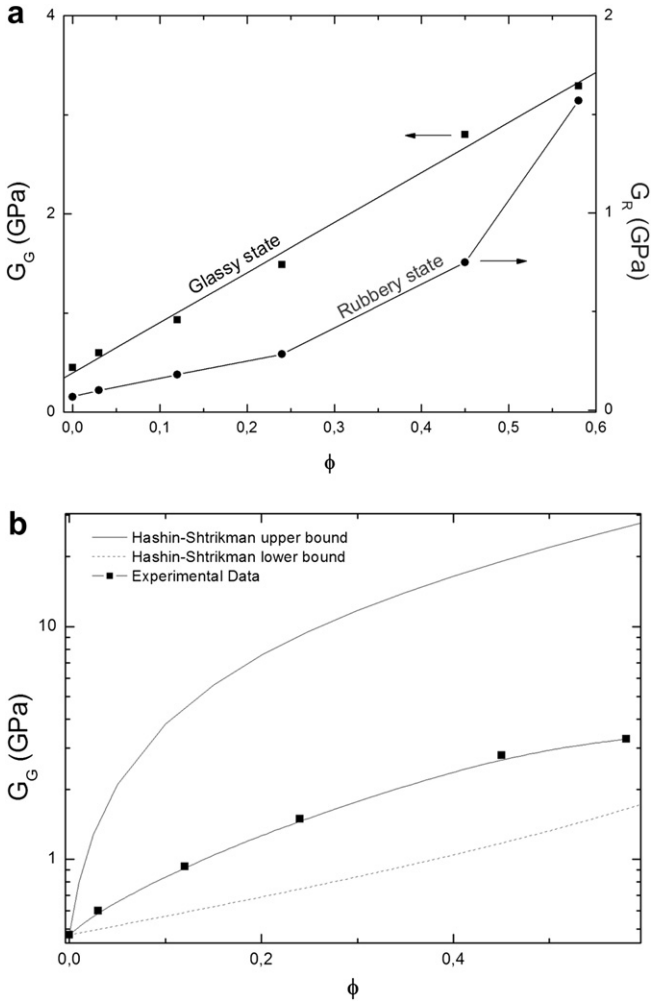

Fig. 6. (a) Storage shear modulus G'_G measured in the glassy state (■) and G'_R in the rubbery state (●) versus volume fraction of $BaTiO_3$ 700 nm; (b) Hashin and Shtrickman upper and lower bounds fitting of experimental G'_G versus the volume fraction of $BaTiO_3$, 700 nm.

transition temperature whatever the fillers content clearly shows that the barium titanate poorly interact with the organic phase. As a consequence, the increase of the cross linking density associated with the densification of the matrix with φ appears to be the relevant parameter. The number-average molecular weight between hydrogen bonds has been extrapolated using a method based on the theory of rubber elasticity [24]. The number-average molecular weight between cross-links M_c is correlated with the rubber plateau modulus according to the equation:

$$M_C = \frac{\rho^* R^* T}{G_R(T)} \tag{2}$$

Where ρ is the polymer density at temperature T, R is the universal gas constant and G_R (T) is the rubbery plateau modulus at temperature T. The value of G_R has been measured at $T = 100$ °C (373 K).

The number-average molecular weight between physical cross-links normalized to the polyamide 11 density (which is a constant value) versus the BT 700 nm volume fraction is reported in Fig. 7. As the content of inorganic phase increases, a significant decrease of the number-average molecular weight between hydrogen bonds is pointed out. A decrease of nearly 1 decade is reported for 58 vol% BT 700 nm. The major parameter acting on the evolution of G_R with φ is the increase of cross-links density due to the densification of the matrix upon increasing of filler content. Fig. 6-a shows that the shear modulus of the viscoelastic state G_R (and as a consequence M_c) is not dependent upon particles size.

3.3. Vitreous plateau

In order to quantify the influence of BT, G' values taken on the vitreous plateau G_G have been reported as function of the volume fraction in Fig. 6-a. G_G increases linearly with the volume content of barium titanate particles; i.e. from 450 MPa for PA11 to 1.49 GPa for 24 vol% and 3.3 GPa for 58 vol%. BT particles increase drastically the value of the glassy plateau. This evolution characterizes a direct stress transfer from matrix to particles. It can be described by the Hashin and Shtrikman model [25] based on the mechanical isotropy and quasi-homogeneity of the composite; i.e. filler dispersed in a homogeneous and isotropic reference material. This model predicts the evolution of the mechanical shear modulus as a function of the volume fraction. Assuming that the ceramic (polymer as particles) or the polymer (ceramic as particles) is taken as matrix the upper (G_c^u) and lower (G_c^l) bounds are calculated respectively as follows:

$$G_c^{\mathrm{u}} = G_{\mathrm{p}} + \frac{1-\phi}{\dfrac{1}{G_{\mathrm{m}}-G_{\mathrm{p}}} + \dfrac{6\phi(K_{\mathrm{p}}+2G_{\mathrm{p}})}{5G_{\mathrm{p}}(3K_{\mathrm{p}}+4G_{\mathrm{p}})}} \tag{3}$$

$$G_c^{\mathrm{l}} = G_{\mathrm{m}} + \frac{\phi}{\dfrac{1}{G_{\mathrm{p}}-G_{\mathrm{m}}} + \dfrac{6(1-)\phi(K_{\mathrm{m}}+2G_{\mathrm{m}})}{5G_{\mathrm{m}}(3K_{\mathrm{m}}+4G_{\mathrm{m}})}} \tag{4}$$

Where φ is the volume fraction of filler in the matrix; K and G are the bulk and shear moduli, the subscripts m and p are related to matrix and particles respectively. In Newnham's notation, the lower and upper bounds can be expressed as 0–3 connectivity (ceramic inclusions homogeneously dispersed in polymer) and 3–0 connectivity (polymer inclusions homogeneously dispersed in a ceramic). For Polyamide 11/$BaTiO_3$ composites, the values of Hashin and Shtrikman parameters are $G_p = 67$ GPa, $K_p = 50$ GPa and $G_m = 400$ MPa, $K_m = 270$ MPa.

A comparison of G_G (φ) with the Hashin and Shtrikman (H–N) model is reported on Fig. 6-b. The experimental values are in the H–N range and close to the H–N lower bound. It is consistent with the fact that barium titanate is stiffer than polyamide. As the increase of G_G follows the lower bound of the H–N model, we assume that the dispersion of the $BaTiO_3$ 700 nm particles is homogeneously dispersed at a macroscopic scale in the polyamide matrix until a volume fraction of 58%.

The conservative part of the shear modulus of PA11/$BaTiO_3$ composites elaborated with 100 nm, 300 nm and 700 nm particles is plotted in Fig. 2. The shear modulus of the composites is higher than the one of PA11. The evolution of G_G with the particles size is different in the glassy (G_G) and in the rubbery state (G_R). G_G decreases of about 130 MPa for particles size decreasing from 700 nm to 100 nm. This observation is in good agreement with the effective interface model [26]: softer organic/inorganic interfaces might explain the decrease of the glassy modulus.

3.4. Viscoelasticity

Figs. 2 and 3 clearly point out that the viscoelastic relaxation temperature T_α is independent from the volume content or the particles size of BT. For the α mode, normalized mechanical losses $G''/G''_{\max}$ are reported on Fig. 8. This representation exhibits the shape evolution of the α peak with φ. The peak dissymmetry increases with the BT volume content. Below $\varphi = 12\%$, this broadening occurs predominantly for the peaks at low temperature; it suggests that BT increases the heterogeneity of the amorphous phase towards regions of higher molecular mobility. Above 12%, the dissymmetry increases on the high temperature side indicating that the high temperature mechanical behaviour is changed for high BT content. The heterogeneity of the amorphous phase can be described by the decrease of the Cooperative Rearranging Regions (CRR) proposed by Adam and Gibbs [27] and adapted to the fitting of DSC data by Donth [28,29].

Decrease of the CRR size upon the introduction of submicronic particles has been exhibited on the same samples, by thermo-stimulated currents [30]. Many authors have reports the influence of the fillers [31] content or crystallinity [32,33] of the samples on the CRR size. In both cases, an increase of non amorphous phase content (inorganic fillers or crystal phase) leads to a decrease of the CRR sizes associated with an increase of the heterogeneity in the amorphous phase of the polymer. The heterogeneity of the

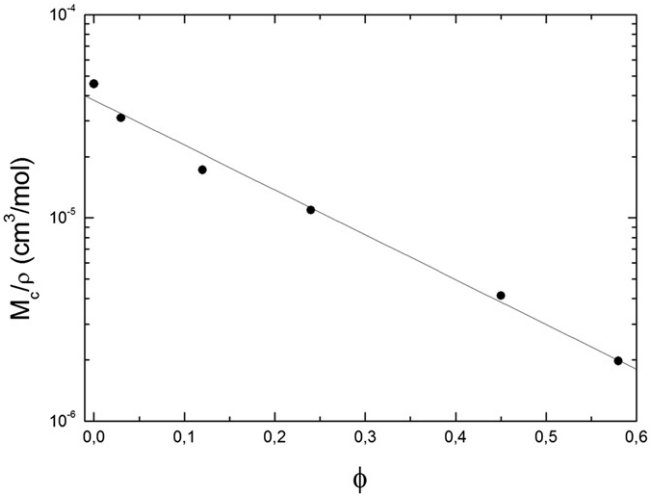

Fig. 7. Number average molecular weight between hydrogen bonds normalized to the polyamide density (M_c/ρ) versus the BT volume fraction calculated at $T = 100$ °C (373 K).

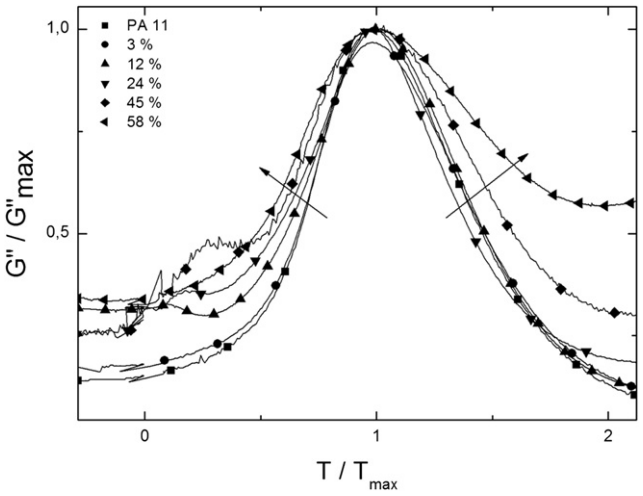

Fig. 8. Normalized dissipative shear modulus G''/G''_{max} of the mechanical α relaxation versus temperature for PA11/$BaTiO_3$, 700 nm.

amorphous phase has been exhibited from the broadening of the structural relaxation observed at T_g by modulated DSC [34]. In PA11/$BaTiO_3$ composites, the decrease of the CRR size cannot be attributed to the crystallinity degree of the polymer. However, inorganic fillers tend to act as crystallites. As the volume fraction of Barium titanate increases, the hydrogen bond density raises leading to a more heterogeneous amorphous phase with smaller CRR sizes.

4. Conclusion

The understanding of PA11/$BaTiO_3$ mechanical behaviour is crucial due to their piezoelectric properties and their potential applications in detection or electromechanical transduction systems. The static and dynamic mechanical behaviour of ferroelectric PA11/$BaTiO_3$ composites has been reported. The influence of $BaTiO_3$ volume fraction has been studied. In the static regime, as the filler loading increases, a change in the mechanical behaviour from ductile to fragile appears for $\varphi > 12\%$ due to a change of connectivity of the inorganic phase. In the dynamic regime, an increase of the shear modulus in the glassy and rubbery plateau is observed upon increasing of the BT content. The volume fraction dependence of the glassy shear modulus is well described by the Hashin and Shtrikman model indicative of a lack of interaction between the organic and inorganic phases. Accordingly, the viscoelastic relaxation temperature is unmodified upon the introduction of BT particles. The broadening of the relaxation reflects an evolution of the physical structure of the amorphous phase. The non linear variation of the rubbery modulus versus particles content follows the rubber elasticity model applied to a hydrogen bond network. Then, the increase of BT content results in an increase of hydrogen bond density that is coherent with the existence of cooperative rearranging regions of smaller size.

Acknowledgements

The authors acknowledge the financial support from DGCIS and Conseil Régional Midi-Pyrénées under NACOMAT contract.

References

[1] Kawai H. Jap J Appl Phys 1969;8:975.
[2] Samara GA, Bauer F. Ferroelectrics 1992;135:385.
[3] Roberts S. Phys Review 1947;71:890.
[4] Furukawa T, Fujino K, Fukada E. Jap J Appl Phys 1976;15:2119.
[5] Dias CJ, Das Gupta DK. IEEE Trans Dielec Elec Ins 1996;3:706.
[6] Newnham RE, Skinner DP, Cross LE. Mat Res Bull 1978;13:525.
[7] Wan T, Clifford MJ, Gao F, Bayley AS, Gregory DH. Polymer 2005;46:6429.
[8] Hu X, Johnson RB, Schlea MR, Kaur J, Shafner ML. Polymer 2010;51:748.
[9] Wenger MP, Das-Gupta DK. Polym Eng Sci 1999;39:1176.
[10] Cross LL. Mat Chem Phys 1996;43:108.
[11] Marra SP, Ramesh KT, Douglas AS. Comp Sci Tech 1999;59:2163.
[12] Fang F, Yang W, Zhang MZ, Whang Z. Comp Sci Tech 2009;69:602.
[13] Capsal JF, Dantras E, Dandurand J, Lacabanne C. J Non-Cryst Solids 2007; 353:4437.
[14] Capsal JF, Dantras E, Dandurand J, Lacabanne C. J Non-Cryst Solids 2010; 356:629.
[15] McCrum NG, Read BE, Williams G. NewYork: John Wiley & Sons; 1967.
[16] Suh DJ, Lim YT, Park OO. Polymer 2000;41:8557.
[17] Xidas PI, Triantafyllidis KS. Eur Polym J 2010;46:404.
[18] Weon JI, Sue HJ. Polymer 2005;46:6325.
[19] Abdalla M, Dean D, Adibempe D, Nyairo E, Robinson P, Thompson G. Polymer 2007;48:5662.
[20] Sun Y, Zhang Z, Moon KS, Wong CP. J Polym Sci Part B 2004;42:3849.
[21] Fragiadakis D, Pissis P. J Non-Cryst Solids 2007;453:4344.
[22] Fragiadakis D, Pissis P, Bokobza L. Polymer 2005;46:6001.
[23] Rittigstein P, Torkelson JM. J Polym Sci Part B 2006;44:2935.
[24] Ferry JD. Viscoelastic properties of polymers. John Wiley & Sons; 1970.
[25] Hashin Z, Shtrikman S. J Mech Phys Sol 1963;11:127.
[26] Odegard GM, Clancy TC, Gates TS. Polymer 2005;46:553.
[27] Adam G, Gibbs JH. J Chem Phys 1965;43:139.
[28] Donth E. J Polym Sci B 1996;34:2881.
[29] Donth E. Acta Polym 1999;50:240.
[30] Sender C, Capsal JF, Lonjon A, Bernes A, Demont P, Dantras E, et al. "Polymer physics: from suspensions to nanocomposites to beyond". John Wiley; 2010.
[31] Khan AN, Hong PD, Chuang WT, Shih KS. Polymer 2009;50:6287.
[32] Delprouve N, Saiter A, Mano JF, Dargent E. Polymer 2008;49:3130.
[33] Lixon C, Delprouve N, Saiter A, Dargent E, Grohens Y. Eur Polym J 2008; 44:3377.
[34] Saiter A, Delprouve N, Dargent E, Saiter JM. Eur Polym J 2007;43:4675.